Shear test on CFRP Full-field measurement and finite element analysis

S. Mistou[a], M. Fazzini[a] and M. Karama[a]

[a] Université de Toulouse, INPT/ENIT, LGP,

avenue d'Azereix, BP1629, F– 65016 Tarbes Cedex, France

marina.fazzini@enit.fr, mistou@enit.fr, moussa@enit.fr

Keywords: Metal-matrix composites; Mechanical properties; Finite element analysis; Mechanical testing

Abstract. The purpose of this work is to study the Iosipescu shear test and more precisely its ability to characterize the shear modulus of a carbone/epoxy composite material. The parameters influencing this identification are the fibre orientation, the geometry of the notch and the boundary conditions. Initially these parameters were studied through the finite element analysis of the shear test. Then, the measurement of the shear strains was carried out by traditional methods of measurement (strain gauges) but also by optical methods. These optical methods: the digital image correlation and the electronic speckle pattern interferometry (ESPI); allow for various levels of loading, to reach a full-field measurement of the shear strain. This enabled us to study the strain distribution on the section between the two notches. The finite element model enabled us to study the parameters influencing the calculation of the shear modulus in comparison with strain gauges, image correlation and ESPI. This work makes it possible to conclude on optimal parameters for the Iosipescu test.

Introduction

Iosipescu proposed in 1967 a testing method of shear strength for metals. The Iosipescu test consists in applying a shear stress on a notched bar, in the shape of a couple, whose purpose is to determine resistance in shearing. The test specimen has two notches of 90°. The depth of each notch is equal to one quarter of the specimen. The experimental device is composed of two antisymmetric identical parts placed on both sides specimen and presented between the heads of the testing device (Fig. 1). Walrath and Adams adapted a new assembly starting from the Iosipescu test which was essential like standard test for composite materials (ASTM) [1, 2, 3].

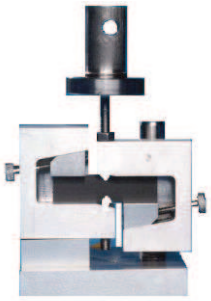

Fig.1. Iosipescu experimental device

Petterson and al [4, 5] have experimentally verified with image correlation that the distribution of the shear field depended on the fibres orientation and was not homogeneous and symmetrical in the central part of the specimen. For the test with 90°, the shear strains are maximum in the centre of the specimen between the notches, they decrease when approaching the notches (Fig. 2-a). For the test with 0°, the shear strains are maximum close to the notches and drop when approaching the centre of the specimen (Fig. 2-b).

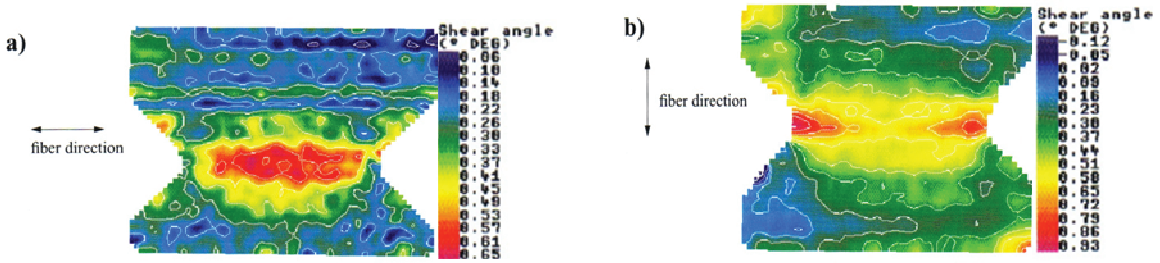

Fig.2. Experimental measurement of strain in the fibre direction a) 90 ° and b) 0°

Hawong and al [6] also showed the influence of the angle of notch on the distribution of the shearing stress field by photoelasticity on an isotropic material (resin). They show thus that for an angle of notch of 110° we obtain a more homogeneous of shear strain field in the centre of the specimen (Fig. 3). Moreover, differences between the theoretical shear stress and the shear stress measured are lower with a specimen whose angle of notch is 110° .

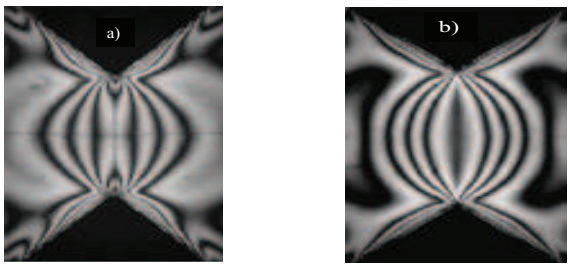

Fig.3. Experimental measurement of strain for to the notch angle of (a) 90° and (b) 110°

Two systems of full-field measurement of displacements and strain are available to the ENIT Laboratory. The image correlation is based on the analysis of grey levels for the measurement of displacement. The measurement of displacements and the calculation of deformations are carried out by Aramis software (GOM). Analysis techniques by image correlation are extremely sensitive; however the threshold for their use must be greater than 0.1% in strain [7-12]. That is why we used in parallel another technique, the ESPI. This technique, based on the speckle interferometry, consists in colouring the surface of measurement in coherent light. The software IstraMs-Q100 by Dantec-Ettemeyer makes possible to calculate displacements then strains [13-15].

Numerical modelling

The purpose of modelling is to create a model that allows us to study the influence of parameters on the calculation of shear modulus. We concluded (based on the bibliography) that the parameters influencing the identification of the shear modulus were related to material characteristics (fibres orientation), the geometry of the specimen (angle of notch) and mode of loading (contact between the clamps and the specimen). The model carried out on Ansys made possible to study these parameters, to find the experimental results, and to conclude on optimal parameters.

Creation of the geometrical model parameterized in Ansys language

The geometrical parameter setting of the specimen is carried out according to figure 4. We vary these parameters to determine their influence on the identification of the shear modulus. We need to create a 2D model in plane stress using the parameters L, h, R, α and d.

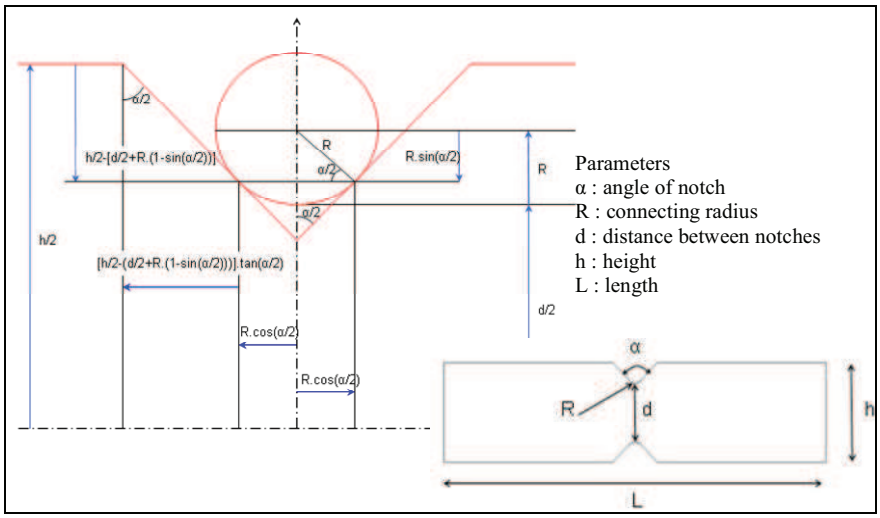

Fig.4. Geometrical parameters of the specimen

Study of convergence

The element retained for the mesh is a quadrilateral with 8 nodes: 2D-PLANE-82. The study focuses on the convergence of shear strain on the central part of the specimen. The mesh is increasingly fine if we approach the centre of the specimen. The result of this study gives a model with 18 000 elements, 55 000 nodes and approximately 110 000 dof (Fig. 5).

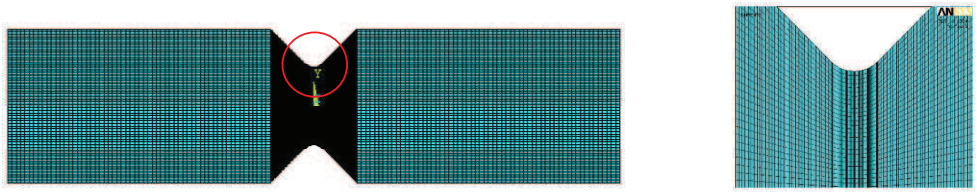

Fig.5. Mesh of the specimen

Optimization of the boundary conditions

The establishment of the boundary conditions of the Iosipescu test is the principal step that requires further investigation. Indeed, it alone determines the result of calculation by finite elements. We will use the same method as that described by Pierron [1] to model the contact between the clamps and the specimen. From the initial boundary conditions we will test the reaction forces and eliminate the boundary conditions that lead to illogical reaction forces. This iterative procedure or macro was developed in the language APDL (Ansys Parametric Design Language).

Our starting point is the model locked in displacement in y direction on the left part of the specimen in top and bottom, and a lock on x in the far left to exclude the rigid body translation in x. On the right side of the specimen, we apply a displacement of 0.1 mm in y direction in top and bottom (Fig. 6-a).

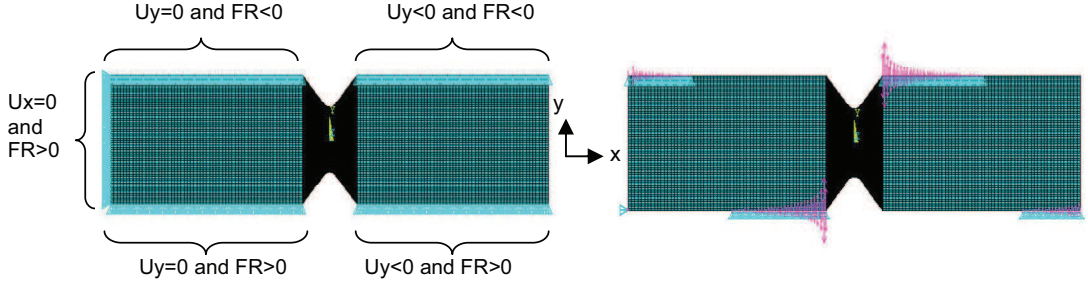

Fig.6. Optimization of the boundary conditions a) original and b) final

After several iterations, we arrive in a stabilized state of the boundary conditions (Fig. 6-b). During the testing process, the macro is used to recover the reaction force at each node and check its sign depending on the orientation of the normal to the side. If the reaction force (FR) indicates that the clamp pulls the specimen (Fig.7), which is impossible as both parts are not united, then the corresponding displacement condition is removed. Moreover the assembly modifies the conditions, there is a shift of the clamps compared to the beginning of V. We chose to study the influence of this shift by creating a parameter m (Fig. 8).

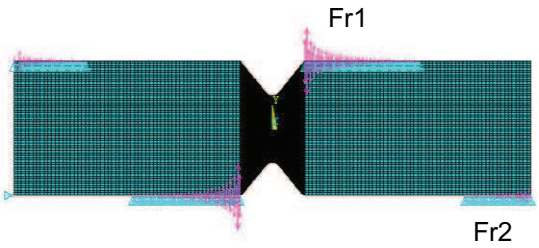

Fig. 7. Exploitation of the shear modulus

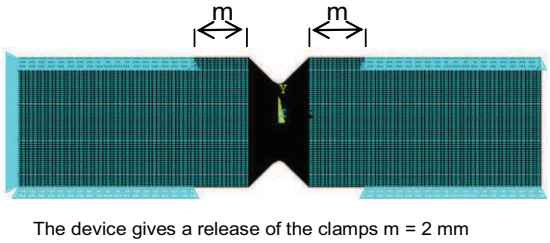

Fig. 8. Release of the clamps

In order to compare the results with non-contact results and traditional methods results (strain gauges), we decided to retrieve the average shear strain over an equivalent area which has the same size of the gauge.

Mechanical characteristics of the composite

They vary according to the orientation of fibres in the specimen. The material is a composite carbon-epoxy. There are three types of reinforcement, two one-way with 0° and 90° and a laminate $[0/90/0/90]_s$. The mechanical properties are given in Table 1.

	E_1 GPa	E_2 GPa	E_3 GPa	G_{12} GPa	G_{13} GPa	G_{23} GPa	ν_{12}	ν_{13}	ν_{23}
 1=0°	170	8	8	4	4	2	0.28	0.28	0.28
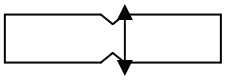 2=90	8	140	8	4	2	4	0.28	0.28	0.28
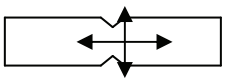 0°/90°	82.5	82.5	8	4	4	4	0.03	0.28	0.28

Table1. Mechanical properties of carbon-epoxy specimens

Study of sensitivity using FE model

The study of sensitivity relates to the various parameters defined above. We present only the results for the orientation of fibres and the angle of the notch. The distance between notches has a significant influence only for the fibre orientation of 0°. Whatever the distance between notches and the release of the clamps, the reinforcement $[0/90/0/90]_s$ is the best compromise for the identification of the shear modulus.

Fibres orientation

We chose to study the influence of the fibres orientation on the geometry of the specimens to compare the experimental results (Fig. 9).

The fibres orientation in the specimen has an influence on the distribution of the shear strain field, on the boundary conditions and on the distribution of the load generated by the contact between the clamps and the specimen. The shear field is antisymmetric for the three fibre orientations.

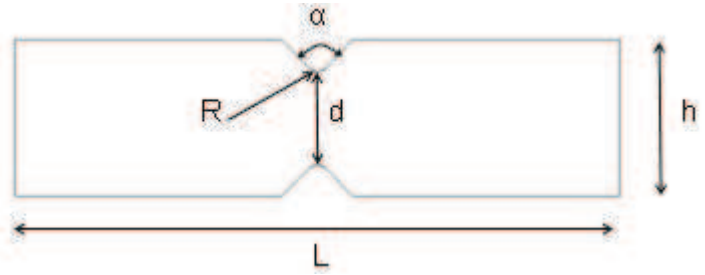

α = 90°	L = 75,1 mm
R = 1,3 mm	m = 2 mm
d = 11,45 mm	e = 2mm
h =19,1 mm	(e : thickness)

Fig.9. Geometry of the specimen

For the reinforcement of 0°, we can see strain concentrations around the connection with the clamps, and shear strain are maximum near the connecting radius (Fig. 10-a) as already seen in the bibliography. Shear strain are maximum at the centre of the specimen for a fibre orientation of 90° and decreases when approaching the notches (Fig. 10-b). The load transmitted by the clamp is distributed much less than for the orientation with 0°. Finally, for the reinforcement $[0/90/0/90]_s$ strains are homogeneous on the sheared section (Fig. 10-c). The load transmitted by the clamp is distributed less than for the orientation 0° and it is more uniform than the orientation 90°.

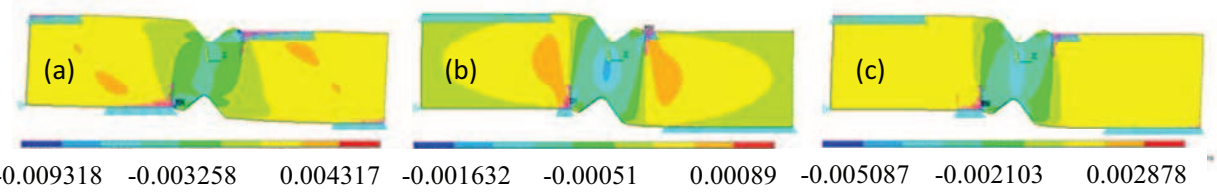

Fig. 10. Strain field for the fibre orientation a) 0° b) 90° c) $[0/90/0/90]_s$

We set the movement to get the same load applied to each fibre orientation (Table 2). The difference between the theoretical module ($G_{xy} = \tau_{xy} / \gamma_{xy}$) and measured module ($G_{xy} = (F/S)/\gamma_{xy}$) allows us to conclude on the optimal fibre orientation for the determination of the shear modulus.

Fibre Orientation (°)	Displacements (mm)	F (N)	S (mm²)	γ_{xy} (m/m)	$G_{xy}=\tau_{xy}/\gamma_{xy}$ (MPa)	$G_{xy}=(F/S)/\gamma_{xy}$ (MPa)	Deviation (%)
0	0,098	300	22,9	0,002864	4000	4574	14,35
90	0,082	300	22,9	0,003579	4000	3661	-8,48
[0/90/0/90]s	0,056	300	22,9	0,003205	4000	4087	2,19

Table 2. Calculation of shear modulus of the fiber orientation

When we calculate the deformation at the centre of the specimen on equivalent zones to gauge sizes Ansys delivers similar results to experimental results recorded by the gauges. With the observation of the distribution of the deformations (Fig. 11) on the sheared section we find the results of the shear modulus calculation (Table 2).

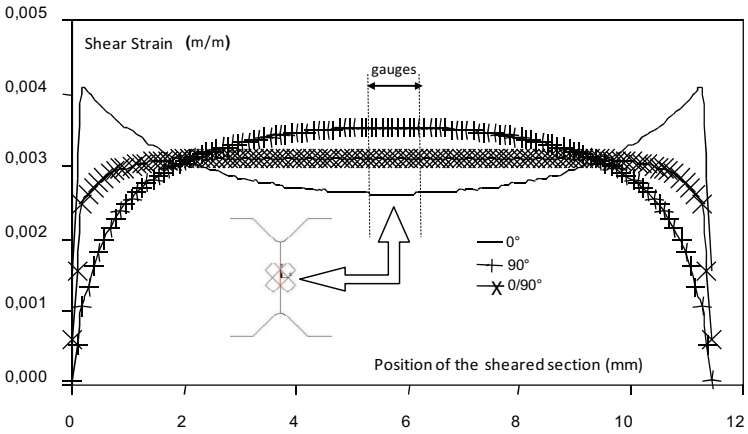

Fig. 11. Strain on the section on the fibre orientation and position of gauges

Shear deformations are distributed differently depending on the fibres orientation (Fig. 11). For the test with 0°, the shear strains are maximum at the notches, they drop when we approach the centre. The shear modulus is then overestimated. For the test with 90°, the shear strains are minimal close to the notches and increase when we approach the centre. The shear modulus is underestimated. The homogenized material $[0/90/0/90]_s$ presents a more homogeneous distribution on the section. The calculated shear modulus is close to the module of the material. This explains the variations in the calculation of the shear modulus when extensometric gauges are used (Table 2). The area under the curves is identical for the three orientations of fibres. The three curves intersect in two points because the evolution curves for fibres oriented 0° and 90° vary in opposition.

Angle of notch

We chose to study the influence of the angle of the notch on the calculation of shear modulus with the geometry of standard specimens by changing only this parameter (Fig. 12). The study is repeated for the three directions 0°, 90°, $[0/90/0/90]_s$.

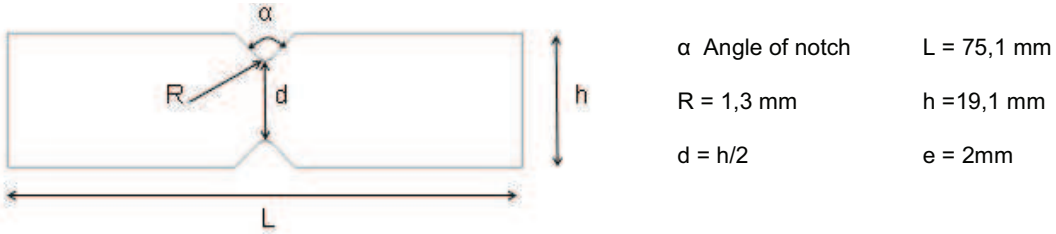

Fig.12. Geometry of the specimen

The purpose of the angle of notch is to locate the shearing strains on the same section. It therefore has a direct influence on the distribution of strains and thus on the measurement results of the shear modulus by the gauges. The variation of the deviation carried out in the calculation of the shear modulus is linear when we vary the angle of notch. We see that it is impossible to define an

angle of notch which would make it possible to reach a null error for all the fibre orientations (Fig. 13). For the orientation $0/90^{\circ}$ the variation is null for an angle of 110° as for isotropic material [6]. For a test-tube with notch 90°, defined by the standard, the best solution is obtained for the reinforcement with $[0/90/0/90]_s$.

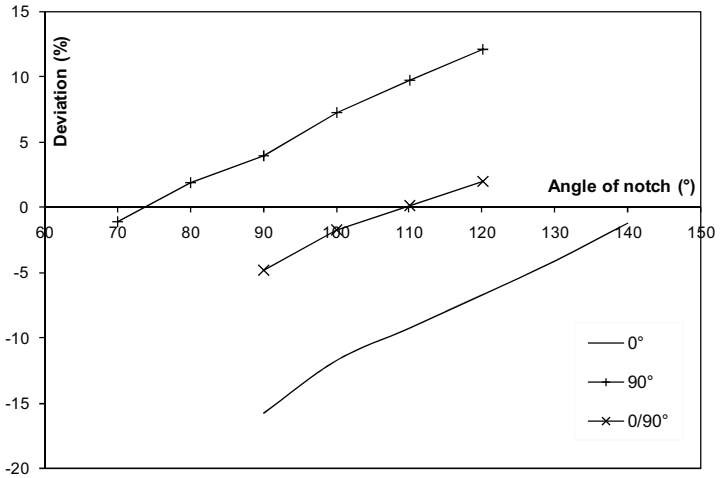

Fig. 13. Deviation of calculation of the shear modulus of the angle of notch

Full field measurements

Two devices of non contact measurement of displacements and strains are available at the Laboratory of ENIT. The first one is based on image stereocorrelation from two numerical cameras. The second one is a device based on the speckle interferometry starting from a laser source. Digital image correlation allows the measurement of displacement fields of a planar surface: a single camera acquires a sequence of images of a planar object under plane strain. Displacements of points on the surface of the object are calculated from the grey level analysis of the images. Given two images corresponding to two deformation states of an object, to determine the correspondent of a point and its signature of the first image in the second, a similarity function is used. Usually, the points are correlated by using a virtual grid that facilitates the calculation of strain from the measured displacements.

From its principle, the correlation technique can function correctly only with objects having a surface with a sufficiently random texture. If the object is not naturally textured or if its texture is not sufficiently discriminating, various techniques exist to al-low the use of correlation: illumination of the surface with a laser source to display a granular structure (speckle effect), paint projection...

Compared to the grid methods, the images correlation has many advantages including facility of preparation of the surface of the object (paint projection in a few seconds), when that is necessary, the density of information obtained (each pixel of the CCD array can be matched by correlation which provides a dense displacement field), the choice of the virtual grid used to calculate the strain from the displacement is carried out at post-processing data and can thus be adapted to the strain gradients. This is one of the biggest advantages of the correlation method compared to grid methods which impose the choice of the step of the grid at the moment of its deposit on the object before strain [6].

Analysis techniques by images correlation are extremely sensitive and allow a very effective mechanical characterization. However, the threshold of their use must be higher than 0.1% in strain [7,8]. This is why we used another optical measurement technique without contact, the ESPI. This

technique, based on the speckle interferometry, consists in colouring the surface of measurement in coherent light on a CCD sensor. Under these conditions a granular structure (speckle), often comparable with noise is superimposed on the image. This structure is the signature or fingerprint of the surface of the sample. When the surface is deformed speckle structure changes and an analysis of its evolution allows measuring the strains (appearance of fringes). The laser beam is split into two similar beams, the first directed by a lens on the measurement surface and the second taken as reference is deviated by a splitter and observed by a CCD camera. The incident beam is reflected (by the measurement surface) and directed by a lens to the CCD camera via the splitter (Fig. 14).

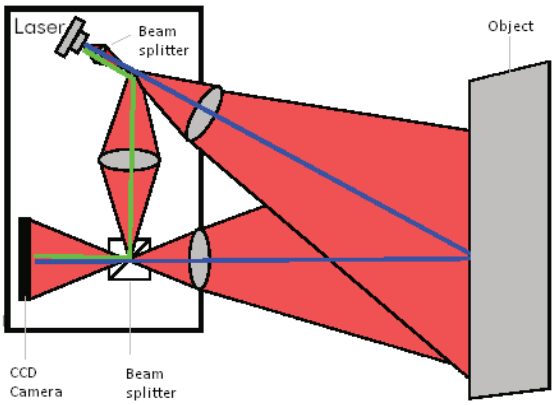

Fig. 14. Principle of ESPI

Experimental device

The tests are carried out on a tensile testing machine Instron by using a special assembly for the Iosipescu specimen carried out by EADS/ST (Fig. 15). The control of the value of the load applied by the tensile testing machine is carried out using the Instron software. The speed applied is $0.5\text{mm}/\text{min}$. A rosette of 3 gauges with 45° is stuck on the central part of the specimen. The acquisition is performed using a data logging system HBM UPM60 controlled by a PC with Catman software. A CCD camera will acquire images that are then analyzed using the Aramis software (correlation). The sensor Q-100 (ESPI) is placed directly on the useful zone of the specimen. For the correlation, an automatic synchronization was carried out from the analogical exit in displacement of the tensile testing machine all the 0.125mm.

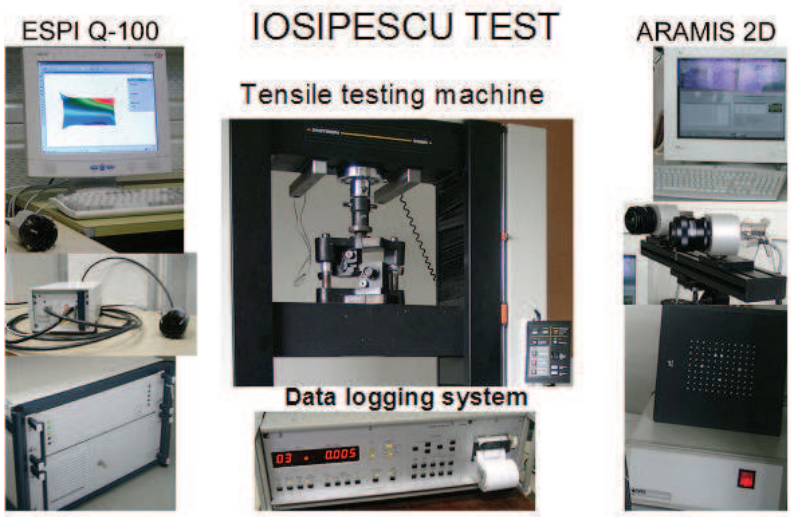

Fig. 15. Testing device

Results of tests (specimen with $0/90^{\circ}$ **)**

On the curves measured by the tensile testing machine (Fig. 16), the three specimens have a similar behaviour with a displacement to the fracture of approximately 3 mm for a load of 2kN. The test was conducted in two phases, a first phase at small strains by manual steps (measurement by gauges and ESPI Q-100) noted "linear" and then a discharge and an increase at constant displacements speed until fracture of the specimen (measurement by gauges until delaminating and correlation Aramis 2D) noted "non-linear".

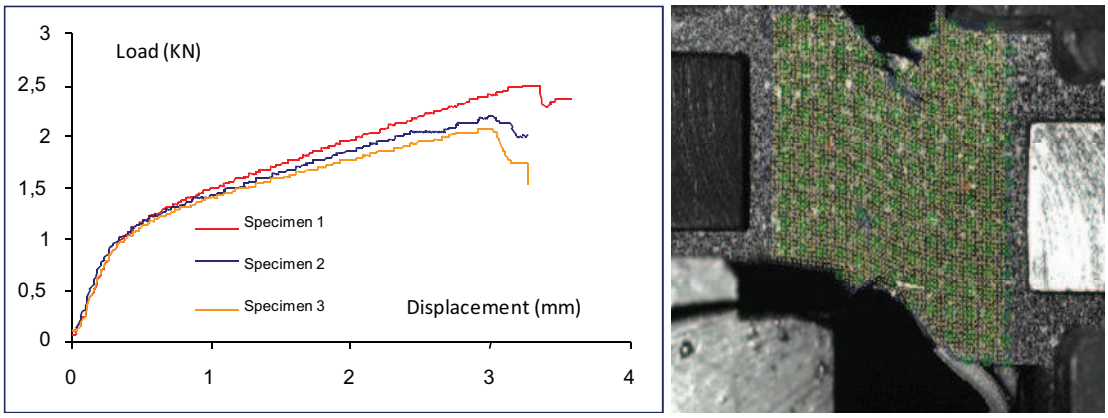

Fig.16. Load-displacement curve for specimen with 0°/90° and picture of the fracture

Linear zone by ESPI

The first part of the test is performed by a displacement carried out manually on the tensile testing machine, imposed by the speckle interferometry system in order to reveal only a dozen fringes per step of displacement. This first part of test is made in small strain. For each test, a retrofit of clearance of approximately 0,6 mm was measured and the corresponding strain determined by ESPI allowed to correct the strain measured thereafter.

	Gauges revised value (310µm/m)	ESPI Q-100 Average		Min		Max	
		Rev. Value (310µm/m)	Deviation (%)	Rev. value (234µm/m)	Deviation (%)	Rev. value (356µm/m)	Deviation (%)
ε_{xy} (µm/m)	3785	3859	2	2490	34	4696	24
γ_{xy} (µm/m)	7570	7718	2	4980	34	9392	24
F (N)				754			
F/A (MPa)				32.78			
G_{xy} (Gpa)	**4.33**	**4.24**	**2**	6.58	52	3.49	19

Table 3. Shear Measurement with ESPI

Table 3 below shows the results for a specimen. This is the difference between the last step and the reference step. The measurement by ESPI is broken up into three values: “Average” corresponding to an average of measurements on a zone (or gauge) of size 5x5 mm equivalent to the strain gauge provided by EADS; “Min” and “max” corresponding respectively to the minimal and maximum value measured on this same zone.

We can note that between the average values corrected of and the shear modulus for ESPI, the error is approximately 2% compared to the gauge (reference). Fig. 17 shows the results of the shear strain obtained by ESPI and more particularly the higher values between the notches (section 0).

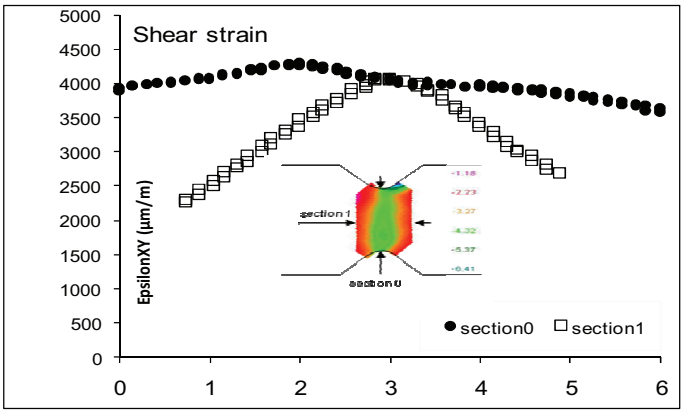

Fig. 17. Shear strain by ESPI

Linear zone by correlation

Table 4 presents the results for the same specimen that tested by interferometry. This is the difference between the first measurement with 0,249 mm and the reference step. The measurement by correlation is decomposed in the same way that for the previous measurement by ESPI (Average, Min, max).

We can note that between the average values corrected of ε_{xy} for ARAMIS (linear zone) the error is approximately 22% compared to the gauge (reference) and for the shear modulus, the error is approximately 16%. Fig. 18-a shows the results of the shear strain obtained by correlation in the linear zone.

	Gauges revised value (310µm/m)	Correlation ARAMIS 2D Average Rev. Value (310µm/m)	Deviation (%)	Min Rev. Value (234µm/m)	Deviation (%)	Max Rev. Value (356µm/m)	Deviation (%)
ε_{xy} (µm/m)	3785	4600	22	3100	18	6200	64
γ_{xy} (µm/m)	7570	9200	22	6200	18	12400	64
Dépl. (mm)	0.213	0.249	16	0.249	16	0.249	16
F (N)	754	769	2	769	2	769	2
F/A (MPa)	32.78	33.43	2	33.43	2	33.43	2
G_{xy} (Gpa)	4.33	3.63	16	5.39	25	2.69	38

Table 4. Measurement of the shear by correlation

Non-linear zone by correlation

The continuation of the second part of the test until fracture brought us to an delaminating of the gauges with approximately 18450 µm/m for a load of 1092 N, whereas the correlation follows up to approximately 34000 µm/m for a load of 1600 N. Table 5 presents the results for a displacement of approximately 0.5 mm.

		Correlation ARAMIS 2D					
	Gauges Value	Average Value	Deviation (%)	Min Value	Deviation (%)	Max Value	Deviation (%)
ε_{xy} (µm/m)	18450	19000	3	13800	25	23600	28
γ_{xy} (µm/m)	36900	38000	3	27600	25	47200	28
Displ. (mm)	0.518	0.501	3	0.501	3	0.501	3
F (N)	1092	1086	0.5	1086	0.5	1086	0.5

Table 5. Measurement of the shear by correlation

We can see that the error for an average value of ε_{xy} by ARAMIS compared to our reference (gauge) is about 3%. Fig. 18-b shows the results of the shear strain obtained by correlation.

- According to the various experimental results observed on the various types of specimen we can conclude on the following points:
- The ESPI can measure very accurately the shear modulus G_{xy} in the case of small strain, i.e. when the deformation is within a range of 1 to 10 000 m/m, with a resolution of about 10 m/m,

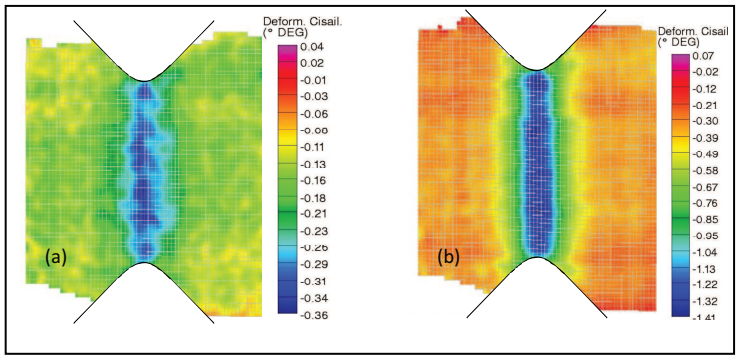

Fig. 18. Shear strain by correlation – a) linear; b): non-linear

- According to the size of the zone (or gauge) on which we carry out an average of the values by ESPI, there may be a difference of 1 to 20% with the value measured by gauge,
- With the digital image correlation, for small strains it is less accurate in the calculation of G_{xy} , the error being about 15% at well as possible, but in the case of large strains the correlation is better adapted for the measurement of slip, i.e. when the strains are in an interval of 1 000 to 200 000 m/m, with a resolution of about 200 µm/m,
- The digital images correlation makes it possible to obtain the shear modulus until the fracture of the specimen (Fig. 19), with more than 200 000 µm/m and 100 MPa which was impossible by technical standards (gauges of extensometry).

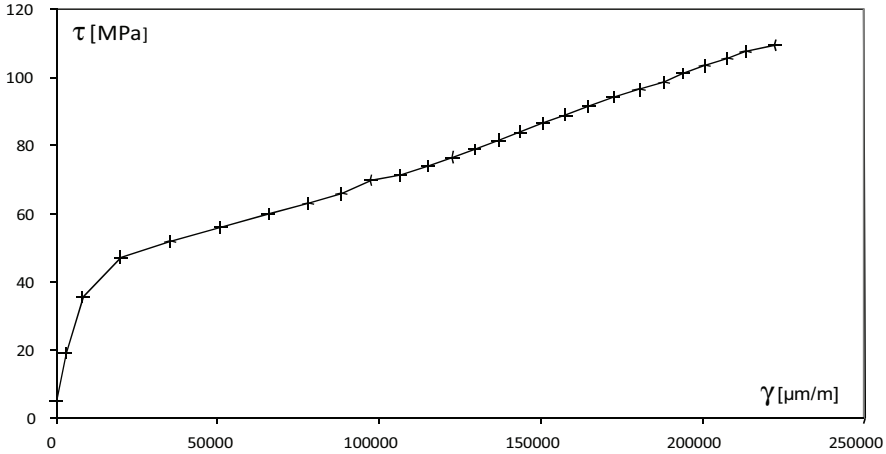

Fig. 19. Shear stress = f (shear strain) DIC

Correlation of the tests and calculations

Calculation of the shear modulus

With the FE model performed on Ansys and previous studies, it is possible to analyze experimental results. Indeed, the tests give a shear modulus different for each fibre orientation. Calculations of shear modulus are made from averages of strain in the zone equivalent to the size of gauge for Ansys and ESPI. Based on the measurement gauges (respectively by ESPI) then we must

enter a shear modulus of 4300 (respectively 4500) MPa in the FE model Ansys to find the same results (Table 6). For fibre orientations of 0° and $[0/90/0/90]_s$ we manages to correlate the calculation and the tests very precisely for the calculation of the shear modulus.

	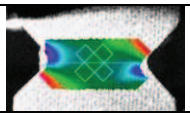	Gauges	Ansys G=4300MPa	Deviation %	ESPI	Ansys G=4500MPa	Deviation %
Shear	0°	4920	4930	0.2	5170	5170	0.02
modulus	90°	4340	3920	9.6	3780	4100	8.4
(Mpa)	$[0/90/0/90]_s$	4370	4370	0.07	4590	4570	0.5

Table 6. Correlation test-calculation

Analysis of the distribution of strain on the section

The optical methods and FE calculating make it possible to analyze the distribution of the strains on the section. We can, while readjusting in load, compare the theoretical distribution with the distribution raised by the ESPI for each specimen. The curves of distribution of strain over the section measured by the ESPI have the same form as the theoretical curve obtained by Ansys for a shear modulus of 4500MPa (Fig. 20).

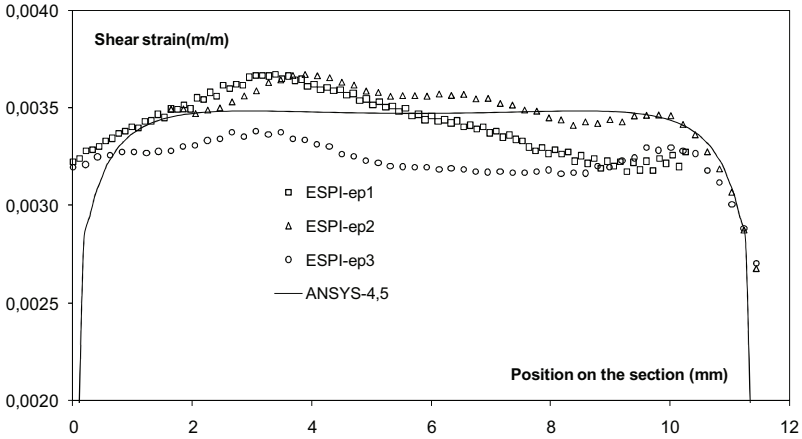

Fig. 20. Distribution of strain on the sheared section $[0/90/0/90]_s$

Conclusion

The finite element model allowed us to study the parameters influencing the calculation of shear modulus. The predominant parameter is the fibres orientation. To determine the shear modulus it is necessary use a composite with a reinforcement $[0/90/0/90]_s$ to reduce the error and dispersions. The orientation 0° gives a good repeatability of the results but the error of measurement of the module is important (15%), this is confirmed by calculation with ANSYS. The orientation 90° gives better results with regard to the error of measurement of the shear modulus that the orientation 0° .

The ESPI results are equivalent to those of the strain gauges although the assembly generated inaccuracies. This method gives access strain on the central part of the specimen, allowing us to study the strain distribution on the section. The finite element model allowed us to understand the differences in calculation caused by gauge measurements between different fibre orientations and to identify the shear modulus of the material (4300 to 4500 MPa).

The FE model also makes it possible to conclude on the optimal parameters of the Iosipescu test:

- Specimen with reinforcement $[0/90/0/90]_s$
- Angle notch

In addition, the digital images correlation used to obtain the shear modulus until the fracture of the specimen, with more than 200 000 μm/m and 100 MPa which was impossible by standard techniques (strain gauges).

Acknowledgements

We acknowledge the EADS SPACE Transportation, Saint-Médard-en-Jalles Centre, for use of their device shear test, for their funding and in-kind contributions of materials and for their additional financial support of this work.

References

[1] Pierron F. L'essai de cisaillement plan d'Iosipescu: modélisation et méthodologie expérimentale pour les composites, Thèse Université Claude Bernard - Lyon I, (1994).

[2] Pierron F., Vautrin A. Measurement of the in-plane shear strengths of unidirectional composites with the Iosipescu test. Composites Science & Technology; 57: 1653-1660, (1997).

[3] Walrath, D.E., Adams, D.F The Iosipescu shear test as applied to composite materials. Experimental Mechanics, 23(1): 105-110, (1983).

[4] Melin L.G., Neumeister J.M., Pettersson K.B., Johansson H. and.Asp L.E. Evaluation of four composite shear test methods by digital speckle strain mapping and fractographic analysis. Journal of Composites Technology & Research; 22(3): 161-172, (2000).

[5] Pettersson K.B. Development of the inclined double notch shear test for determination of interlaminar properties of composite laminates, Thesis KTH Stockholm, (2002).

[6] Hawong J.S., Shin D.C., Baek U.C. Validation of pure shear test device using finite element method and experimental methods, School of Mechanical Engineering (South Korea), (2003).

[7] Karama M., Mistou S., Peres P., Gohorianu G. Mesure de déformations sans contact sur des composites carbone/carbone à architecture 3D. In: Troisième colloque francophone sur les méthodes et technique optiques pour l'industrie, Saint Aubin de Médoc, Novembre, (2002).

[8] Mistou S., Karama M., Desmars B., Peres P., Piron E. Application de la méthode de stéréo-corrélation d'images à la caractérisation des élastomères en grandes déformations. In: Colloque Photomécanique. Ecole des Mines d'Albi-Carmaux, 4-6 Mai (2004).

[9] Sutton M.A., Wolters W.J., Perters W.H., Ranson W.F. and McNeill S.R. Determination of displacements using an improved digital correlation method. Image Vis Comput,1 (3): 133–139, (1983).

[10] Launay J., Lahmar F., Boisse P. and Vacher P. Strain measurement in tests on fibre fabric by image correlation method. Adv Compos Lett,11 (1): 7–12 Adcotec Ltd, (2002).

[11] Bruno L., Furgiuele F. M. Pagnotta L. and Poggialini A. A full-field approach for the elastic characterization of anisotropic materials. Optics Lasers Eng., 37: 417–431, (2002).

[12] Bonnet M, Bui H.D., Constantinescu A. Principes variationnels et exploitation de mesures de champs en élasticité/variational principles and exploitation of field measurements in elasticity. Mécanique et Industries, 4: 687–97, (2003).

[13] Mistou S., Karama M., Cazajus V., Desmars B.et Peres P. Mesure par ESPI des déformations en cisaillement de type compression à double entaille sur des composites carbone. In: Cinquième colloque francophone sur les méthodes et techniques optiques pour l'industrie. Saint Etienne, Novembre (2004).

[14] Ettermeyer A., Wang Z. and Walz T. Application of 3D speckle interferometry to material and component testing. In: Proceedings of SPIE, 188–94, (1997).

[15] Waldner S and Kress G. Nondestructive testing of composite materials with electronic speckle pattern interferometry. In: Rastogi P. and Inaudi D., Editors, Trends. In: optical non-destructive testing and inspection, Elsevier, Amsterdam 2000.Dj.M. Maric, P.F. Meier and S.K. Estreicher: Mater. Sci. Forum Vol. 83-87, p. 119(1992).